

AvatarGen: a 3D Generative Model for Animatable Human Avatars

Jianfeng Zhang^{1*}, Zihang Jiang^{1*}, Dingdong Yang², Hongyi Xu², Yichun Shi²,
Guoxian Song², Zhongcong Xu¹, Xinchao Wang¹, Jiashi Feng²

¹National University of Singapore ²ByteDance

Abstract

Unsupervised generation of clothed virtual humans with various appearance and animatable poses is important for creating 3D human avatars and other AR/VR applications. Existing methods are either limited to rigid object modeling, or not generative and thus unable to synthesize high-quality virtual humans and animate them. In this work, we propose AvatarGen, the first method that enables not only non-rigid human generation with diverse appearance but also full control over poses and viewpoints, while only requiring 2D images for training. Specifically, it extends the recent 3D GANs to clothed human generation by utilizing a coarse human body model as a proxy to warp the observation space into a standard avatar under a canonical space. To model non-rigid dynamics, it introduces a deformation network to learn pose-dependent deformations in the canonical space. To improve geometry quality of the generated human avatars, it leverages signed distance field as geometric representation, which allows more direct regularization from the body model on the geometry learning. Benefiting from these designs, our method can generate animatable human avatars with high-quality appearance and geometry modeling, significantly outperforming previous 3D GANs. Furthermore, it is competent for many applications, *e.g.*, single-view reconstruction, reanimation, and text-guided synthesis. Code and pre-trained model will be available.

1 Introduction

Generating diverse and high-quality virtual humans (avatars) with full control over their pose and viewpoint is a fundamental but extremely challenging task. Solving this task will benefit many applications like immersive photography visualization [69], virtual try-on [32], VR/AR [62, 22] and creative image editing [68, 19].

Conventional solutions rely on classical graphics modeling and rendering techniques [9, 7, 12, 56] to create avatars. Though offering high-quality, they typically require pre-captured templates, multi-camera systems, controlled studios, and long-term works of artists. In this work, we aim to make virtual human avatars widely accessible at low cost. Towards this goal, we propose the first 3D-aware avatar generative model that can *generate* 1) high-quality virtual humans with 2) various appearance styles, arbitrary poses and viewpoints, 3) and be trainable from only 2D images, thus largely alleviating the effort to create virtual human.

The 3D-aware generative models have recently seen rapid progress, fueled by introducing implicit neural representation (INR) methods [6, 43, 36, 37] into generative adversarial networks [3, 40, 42, 16, 2]. However, these models are limited to relatively simple and rigid objects, such as human faces and cars, and mostly fail to generate clothed human avatars whose appearance is highly sundry because of their articulated poses and great variability of clothing. Besides, they have limited control over the

*Equal contribution.



Figure 1: Our AvatarGen model can generate clothed avatars with diverse appearance from arbitrary poses and viewpoints (top), animate the avatars with specific pose signals (middle) and inverse 2D human images into animatable 3D avatars (bottom).

generation process and thus cannot animate the generated objects, *i.e.*, driving the objects to move by following certain instructions. Another line of works leverage INRs [37] to learn articulated human avatars for reconstructing a single subject from one’s multi-view images or videos [47, 41, 63, 5, 48]. While being able to animate the avatars, these methods are *not generative* and cannot synthesize novel identities and appearances.

Aiming at generative modeling of animatable human avatars, we propose AvatarGen, the first model that can generate *novel* human avatars with full control over their poses and appearances. Our model is built upon EG3D [2], a recent method that can generate high quality 3D-aware human faces via introducing a new tri-plane representation method. However, EG3D is not directly applicable for clothed avatar generation because it cannot handle the challenges in modeling complex garments, texture, and the articulated body structure with various poses. Moreover, EG3D has limited control capability and thus it hardly animates the generated objects.

To address these challenges, we propose to decompose the clothed avatar generation into *pose-guided canonical mapping* and *canonical avatar generation*. Guided by a parametric human body model (*e.g.*, SMPL [34]), our method warps each point in the observation space with a specified pose to a standard avatar with a fixed pre-defined pose in a canonical space via an inverse-skinning transformation [20]. To accommodate the non-rigid dynamics between the observation and canonical spaces (like clothes deformation), our method further trains a deformation module to predict the proper residual deformation. As such, our method can generate arbitrary avatars in the observation space by deforming the canonical one which is much easier to generate and shareable across different instances, thus largely alleviating the learning difficulties and achieving better appearance and geometry modeling. Meanwhile, this formulation by design enables *disentanglement between the pose and appearance*, offering independent control over them.

Although the aforementioned method can generate 3D human avatars with reasonable geometry, we find it tends to produce noisy surfaces due to the lack of constraints on the learned geometry (density field). Inspired by recent works on neural implicit surface [59, 66, 42, 48], we propose to use a signed distance field (SDF) to impose stronger *geometry-aware guidance* for the model training. Compared with the density field, SDF gives a better-defined surface representation, which facilitates more direct regularization on learning the avatar geometries. Moreover, the model can leverage the coarse body model from SMPL to infer reasonable signed distance values, which greatly improves quality of the clothed avatar generation and animation. The SDF-based volume rendering techniques [59, 66, 42] are used to render the low resolution feature maps, which are further decoded to high-resolution images with the StyleGAN generator [26, 2].

As shown in Fig. 1, trained from 2D images without using any multi-view or temporal information and 3D geometry annotations, AvatarGen can generate a large variety of clothed human with diverse

appearances under arbitrary poses and viewpoints. We evaluate it quantitatively, qualitatively, and through a perceptual study; it strongly outperforms previous state-of-the-art methods. Moreover, we demonstrate it on several applications, like single-view 3D reconstruction and text-guided synthesis.

Our contributions are threefold. 1) To our best knowledge, AvatarGen is the first model able to generate a large variety of animatable clothed human avatars without requiring multi-view, temporal or 3D annotated data. 2) We propose a human generation pipeline that achieves accurate appearance and geometry modeling, with full control over the pose and appearance. 3) We demonstrate state-of-the-art 3D-aware human image synthesis on several benchmarks along with high-quality geometry.

2 Related Works

Generative 3D-aware image synthesis. Generative adversarial networks (GANs) [15] have recently achieved photo-realistic image quality for 2D image synthesis [23, 25, 26, 24]. Extending these capabilities to 3D settings has started to gain attention. Early methods combine GANs with voxel [61, 38, 39], mesh [57, 30] or point cloud [1, 29] representations for 3D-aware image synthesis. Recently, several methods represent 3D objects by learning an implicit neural representation (INR) [54, 3, 40, 2, 42, 16, 10]. Among them, some methods use INR-based model as generator [54, 3, 10], while some others combine INR generator with 2D decoder for higher-resolution image generation [40, 16, 65]. Follow-up works like EG3D [2] proposes an efficient tri-plane representation to model 3D objects, StyleSDF [42] replaces density field with SDF for better geometry modeling and Disentangled3D [58] represents objects with a canonical volume along with deformations to disentangle geometry and appearance modeling. However, such methods are typically not easily extended to non-rigid clothed humans due to the complex pose and texture variations. Moreover, they have limited control over the generation process, making the generated objects hardly be animated. Differently, we study the problem of 3D implicit generative modeling of clothed human, allowing free control over the poses and appearances.

3D human reconstruction and animation. Traditional human reconstruction methods require complicated hardware that is expensive for daily use, such as depth sensors [7, 12, 56] or dense camera arrays [9, 17]. To reduce the requirement on the capture device, some methods train networks to reconstruct human models from RGB images with differentiable renderers [64, 14]. Recently, neural radiance fields [37] employ the volume rendering to learn density and color fields from dense camera views. Some methods augment neural radiance fields with human shape priors to enable 3D human reconstruction from sparse multi-view data [49, 5, 63, 55]. Follow-up improvements [47, 4, 31, 48, 60] are made by combining implicit representation with the SMPL model and exploiting the linear blend skinning techniques to learn animatable 3D human modeling from temporal data. However, these methods are not generative, *i.e.*, they cannot synthesize novel identities and appearances. In this work, we learn fully generative modeling of human avatars from only 2D images, largely alleviating the cost to create virtual humans.

3 Method

Our goal is to build a generative model for diverse clothed 3D human avatar generation with varying appearances in arbitrary poses. The model is trained from 2D images without using multi-view or temporal information and 3D scan annotations. Its framework is summarized in Fig. 2.

3.1 Overview

Problem formulation. We aim to train a 3D generative model G for geometry-aware human synthesis. Following EG3D [2], we associate each training image with a set of camera parameters \mathbf{c} and pose parameters \mathbf{p} (in SMPL format [34]), which are obtained from an off-the-shelf pose estimator [27]. Given a random latent code \mathbf{z} sampled from Gaussian distribution, and a new camera \mathbf{c} and pose \mathbf{p} as conditions, the generator G can synthesize a corresponding human image $I = G(\mathbf{z}|\mathbf{c}, \mathbf{p})$. We optimize G with a discriminator D via adversarial training.

Framework. Fig. 2 illustrates the framework of our proposed generative model. It takes camera parameters and SMPL parameters (specifying the generated pose) as inputs and generates 3D human avatar and its 2D images accordingly. Our model jointly processes the random canonical code

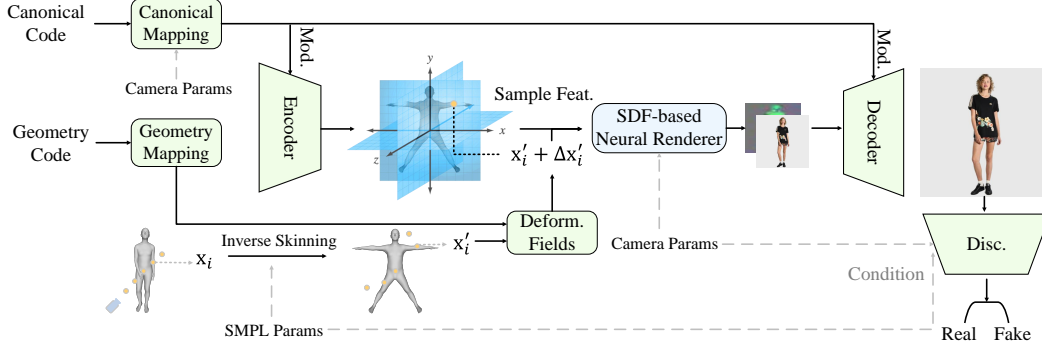


Figure 2: Pipeline of AvatarGen. Taking the canonical code and camera parameters as input, the encoder generates tri-plane based features of a canonical posed human avatar. The geometry code is applied to modulate the deformation field module which deforms the sampled points in the observation space to the canonical space under the guidance of the pose condition (SMPL parameters). The deformed spatial positions are used to sample features on the tri-plane, which are then rendered as low-resolution features and images using the SDF based neural renderer. Finally, the decoder decodes the feature images to high resolution images. The generator with is optimized a camera and pose conditioned discriminator via adversarial training.

and camera parameters by a canonical mapping module (implemented by an MLP) to generate the intermediate latent code that modulates the convolution kernels of the encoder. This encoder then generates a tri-plane based features [2] corresponding to a canonical pose representation. Regarding the pose control, our model first jointly processes a random geometry code and the input pose condition via an MLP-based geometry mapping module, and outputs latent features. Then, given a spatial point \mathbf{x} in the observation space, the output latent features are processed by a deformation field module, generating non-rigid residual deformation $\Delta\mathbf{x}'$ over the inverse skinned point \mathbf{x}' in the canonical space. We sample the features from the tri-plane according to the deformed spatial position $\mathbf{x}' + \Delta\mathbf{x}'$, which are then transformed into appearance prediction (i.e., color features) and geometry prediction (i.e., SDF-based features) for volume rendering. We will explain these steps in details in the following sections.

3.2 Representations of 3D Avatars

It is important to choose an efficient approach to represent 3D human avatars. The recent EG3D [2] introduces a memory-efficient tri-plane representation for 3D face modeling. It explicitly stores features on three axis-aligned orthogonal planes (called tri-planes), each of which corresponds to a dimension within the 3D space. Thus, the intermediate features of any point of a 3D face can be obtained via simple lookup over the tri-planes, making the feature extraction much more efficient than NeRF that needs to forward all the sampled 3D points through MLPs [37]. Besides, the tri-plane representation effectively decouples the feature generation from volume rendering, and can be directly generated from more efficient CNNs instead of MLPs.

Considering these benefits, we also choose the tri-plane representation for 3D avatar modeling. However, we found directly adopting it for clothed human avatars generation results in poor quality. Due to the much higher degrees of freedom of human bodies than faces, it is very challenging for the naive tri-plane representation model to learn pose-dependent appearance and geometry from only 2D images. We thus propose the following new approaches to address the difficulties.

3.3 Generative 3D Human Modeling

There are two main challenges for 3D human generation. The first is how to effectively integrate pose condition into the tri-plane representations, making the generated human pose fully controllable and animatable. One naive way is to combine the pose condition \mathbf{p} with the latent codes \mathbf{z} and \mathbf{c} directly, and feed them to the encoder to generate tri-plane features. However, such naive design cannot achieve high-quality synthesis and animation due to limited pose diversity and insufficient geometry supervision. Besides, the pose and appearance are tightly entangled, making independent

control impossible. The second challenge is that learning pose-dependent clothed human appearance and geometry from 2D images only is highly under-constrained, making the model training difficult and generation quality poor.

To tackle these challenges, our AvatarGen decomposes the avatar generation into two steps: *pose-guided canonical mapping* and *canonical avatar generation*. Specifically, AvatarGen uses SMPL model [34] to parameterize the underlying 3D human body. With a pose parameterization, AvatarGen can easily deform a 3D point \mathbf{x} within the observation space with pose \mathbf{p}_o to a canonical pose \mathbf{p}_c (an “X”-pose as shown in Fig. 2) via Linear Blend Skinning [21]. Then, AvatarGen learns to generate the appearance and geometry of human avatar in the canonical space. The canonical space is shared across different instances with a fixed template pose \mathbf{p}_c while its appearance and geometric details can be varied according to the latent code \mathbf{z} , leading to generative human modeling.

Such a task factorization scheme facilitates learning of a generative canonical human avatars and effectively helps the model generalize to unseen poses, achieving animatable clothed human avatars generation. Moreover, it by design disentangles pose and appearance information, making independent control over them feasible. We now elaborate on the model design for these two steps.

Pose-guided canonical mapping. We define the human 2D image with SMPL pose \mathbf{p}_o as the *observation* space. To relieve learning difficulties, our model attempts to deform the observation space to a *canonical* space with a predefined template pose \mathbf{p}_c that is shared across different identities. The deformation function $T : \mathbb{R}^3 \mapsto \mathbb{R}^3$ thus maps spatial points \mathbf{x}_i sampled in the observation space to \mathbf{x}'_i in the canonical space.

Learning such a deformation function has been proved effective for dynamic scene modeling [45, 50]. However, learning to deform in such an implicit manner cannot handle large articulation of humans and thus hardly generalizes to novel poses. To overcome this limitation, we use the SMPL model to explicitly guide the deformation [31, 47, 4]. SMPL defines a skinned vertex-based human model $(\mathcal{V}, \mathcal{W})$, where $\mathcal{V} = \{\mathbf{v}\} \in \mathbb{R}^{N \times 3}$ is the set of N vertices and $\mathcal{W} = \{\mathbf{w}\} \in \mathbb{R}^{N \times K}$ is the set of the skinning weights assigned for the vertex w.r.t. K joints, with $\sum_j w_j = 1, w_j \geq 0$ for every joint.

We use the inverse-skinning (IS) transformation to map the SMPL mesh in the observation space with pose \mathbf{p} into the canonical space [20]:

$$T_{\text{IS}}(\mathbf{v}, \mathbf{w}, \mathbf{p}) = \sum_j w_j \cdot (R_j \mathbf{v} + \mathbf{t}_j), \quad (1)$$

where R_j and \mathbf{t}_j are the rotation and translation at each joint j derived from SMPL with pose \mathbf{p} .

Such formulation can be easily extended to any spatial points in the observation space by simply adopting the same transformation from the nearest point on the surface of SMPL mesh. Formally, for each spatial points \mathbf{x}_i , we first find its nearest point \mathbf{v}^* on the SMPL mesh surface as $\mathbf{v}^* = \arg \min_{\mathbf{v} \in \mathcal{V}} \|\mathbf{x}_i - \mathbf{v}\|_2$. Then, we use the corresponding skinning weights \mathbf{w}^* to deform \mathbf{x}_i to \mathbf{x}'_i in the canonical space as:

$$\mathbf{x}'_i = T_o(\mathbf{x}_i | \mathbf{p}) = T_{\text{IS}}(\mathbf{x}_i, \mathbf{w}^*, \mathbf{p}). \quad (2)$$

Although the SMPL-guided inverse-skinning transformation can help align the rigid skeleton with the template pose, it lacks the ability to model the pose-dependent deformation, like cloth wrinkles. Besides, different identities may have different SMPL shape parameters \mathbf{b} , which likely leads to inaccurate transformation.

To alleviate these issues, AvatarGen further trains a deformation network to model the residual deformation to complete the fine-grained geometric deformation and to compensate the inaccurate inverse-skinning transformation by

$$\Delta \mathbf{x}'_i = T_{\Delta}(\mathbf{x}'_i | \mathbf{w}, \mathbf{p}, \mathbf{b}) = \text{MLPs}(\text{Concat}[\text{Embed}(\mathbf{x}'_i), \mathbf{w}, \mathbf{p}, \mathbf{b}]), \quad (3)$$

where \mathbf{w} is the canonical style code mapped from the input latent code \mathbf{z} . We concatenate it with the embedded \mathbf{x}'_i and SMPL pose \mathbf{p} and shape \mathbf{b} parameters and feed them to MLPs to yield the residual deformation. The final pose-guided deformation $T_{o \rightarrow c}$ from the observation to canonical spaces can be formulated as

$$T_{o \rightarrow c}(\mathbf{x}_i) = \mathbf{x}'_i + \Delta \mathbf{x}'_i = T_o(\mathbf{x}_i | \mathbf{p}) + T_{\Delta}(T_o(\mathbf{x}_i | \mathbf{p}) | \mathbf{w}, \mathbf{p}, \mathbf{b}). \quad (4)$$

Canonical avatar generation. After deforming 3D points sampled in the observation space to the canonical space, we apply AvatarGen with the tri-plane representation for canonical avatar generation.

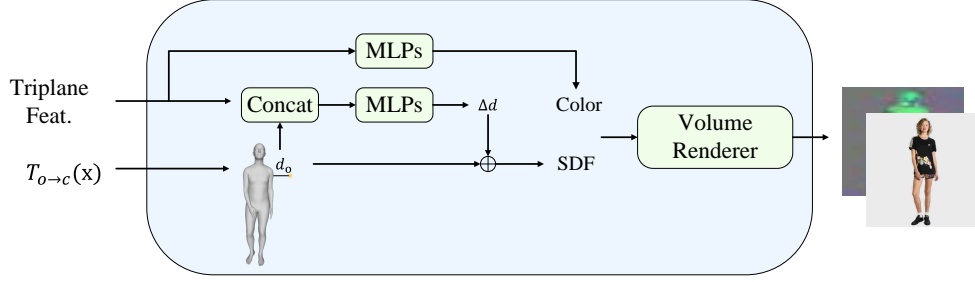


Figure 3: Our proposed geometry-aware human modeling module. It first predicts color and SDF values using the sampled tri-plane features and corresponding point location in the canonical space. Then it feeds them to volume renderer module to generate the raw image and features. The color for each sampled point is directly predicted from the tri-plane feature with MLPs. We use the SMPL model to guide the prediction of SDF and obtain a coarse signed distance value d_o which is concatenated with the input tri-plane feature for predicting the residual distance Δd . The final SDF is $d_o + \Delta d$. See 3.4 for more details.

More concretely, it first generates tri-plane via a StyleGAN generator by taking the latent code \mathbf{z} and camera parameters \mathbf{c} as inputs. Then, for each point deformed via SMPL parameters \mathbf{p} in the canonical space, the model queries tri-plane to obtain the intermediate feature and maps it to color-based feature c and density σ for volume rendering. As such, it generates clothed human appearance and geometry in the canonical space with a predefined canonical pose, which alleviates the optimization difficulties and substantially helps our learning of high-quality avatar generation with disentangled pose and appearance control.

3.4 Geometry-aware Human Modeling

To improve geometry modeling of AvatarGen, inspired by recent neural implicit surface works [59, 66, 42, 48], we adopt signed distance field (SDF) instead of density field as our geometry proxy, because it introduces more direct geometry regularization and guidance. To achieve this, our model learns to predict signed distance value rather than density in tri-plane for volume rendering.

SMPL-guided geometry learning. Although SDF has a well-defined surface representation and introduces several regularization for geometry learning, how to use it for generative human modeling is still non-trivial due to the complicated body articulation and pose-dependent deformation. We therefore leverage the SMPL model as a guidance for the geometry-aware generation and combine it with a residual SDF network (as shown in Fig. 3), that models the surface details (including hair and clothing) not represented by SMPL.

Specifically, given the input SMPL pose \mathbf{p}_o and shape \mathbf{b}_o , we generate a SMPL mesh $M = T_{\text{SMPL}}(\mathbf{p}_o, \mathbf{b}_o)$, where T_{SMPL} is the SMPL transformation function. For each 3D point \mathbf{x} in the observation space, we first obtain its coarse signed distance value d_o by querying the SMPL mesh M . Then, we feed d_o along with the features from tri-plane to a light-weight MLP to predict the residual SDF Δd . The signed distance value of each point is computed as $d = d_o + \Delta d$. Predicting SDF with the coarse SMPL as guidance improves geometry learning of the model, thus achieving better human generation and animation, as demonstrated in our experiments. We also introduce a SMPL-guided regularization for SDF learning as elaborated in Sec. 3.5.

SDF-based volume rendering. Following [42], we adopt SDF-based volume rendering to obtain the final output images. For any point x on the sampled rays, we first deform it to $\bar{x} = T_{o \rightarrow c}(x)$ by pose-guided canonical mapping. We query feature vector $F(\bar{x})$ for position \bar{x} from the canonical tri-plane and then feed it into two MLP layers to predict the color feature $c = \text{MLP}_c(F(\bar{x}))$ and the signed distance $d = d_o + \Delta d = d_o + \text{MLP}_d(F(\bar{x}), d_o)$. We then convert the signed distance value d_i of each point \mathbf{x}_i along a ray r to density value σ_i as $\sigma_i = \frac{1}{\alpha} \cdot \text{Sigmoid}(\frac{-d_i}{\alpha})$, where $\alpha > 0$ is a learnable parameter that controls the tightness of the density around the surface boundary. By

integration along the ray r we can get the corresponding pixel feature as

$$I(r) = \sum_{i=1}^N \left(\prod_{j=1}^{i-1} e^{-\sigma_j \cdot \delta_j} \right) \cdot (1 - e^{-\sigma_i \cdot \delta_i}) \cdot c_i, \quad (5)$$

where $\delta_i = \|\mathbf{x}_i - \mathbf{x}_{i-1}\|$. By aggregating all rays, we can get the entire image feature which is then feed into a StyleGAN decoder [26] to generate the final high-resolutions synthesized image.

3.5 Training

We use the non-saturating GAN loss L_{GAN} [26] with R1 regularization L_{Reg} [15, 35] to train our model end-to-end. We also adopt the dual-discriminator proposed by EG3D [2]. It feeds both the rendered raw image and the decoded high-resolution image into the discriminator for improving consistency of the generated multi-view images. To obtain better controllability, we feed both SMPL pose parameters \mathbf{p} and camera parameters \mathbf{c} as conditions to the discriminator for adversary training. To regularize the learned SDF, we apply eikonal loss to the sampled points as:

$$L_{\text{Eik}} = \sum_{\mathbf{x}_i} (\|\nabla d_i\| - 1)^2, \quad (6)$$

where \mathbf{x}_i and d_i denote the sampled point and predicted signed distance value, respectively. Following [42], we adopt a minimal surface loss to encourage the model to represent human geometry with minimal volume of zero-crossings. It penalizes the SDF value close to zero:

$$L_{\text{Minsurf}} = \sum_{\mathbf{x}_i} \exp(-100d_i). \quad (7)$$

To make sure the generated surface is consistent with the input SMPL model, we incorporate the SMPL mesh as geometric prior and guide the generated surface to be close to the body surface. Specifically, we sample vertices $\mathbf{v} \in \mathcal{V}$ on the SMPL body surface and then use it as query to deform to canonical space and sample features from the generated tri-plane and minimize the signed distance.

$$L_{\text{SMPL}} = \sum_{\mathbf{v} \in \mathcal{V}} \|\text{MLP}_d(F(T_{o \rightarrow c}(\mathbf{v})))\|. \quad (8)$$

The overall loss is finally formulated as

$$L_{\text{total}} = L_{\text{GAN}} + \lambda_{\text{Reg}} L_{\text{Reg}} + \lambda_{\text{Eik}} L_{\text{Eik}} + \lambda_{\text{Minsurf}} L_{\text{Minsurf}} + \lambda_{\text{SMPL}} L_{\text{SMPL}}, \quad (9)$$

where λ_* are the corresponding loss weights.

4 Experiments

We study the following four questions in our experiments. 1) Is AvatarGen able to generate 3D human avatars with realistic appearance and geometry? 2) Is AvatarGen effective at controlling human avatars poses? 3) How does each component of our AvatarGen model take effect? 4) Does AvatarGen enable downstream applications, like single-view 3D reconstruction and text-guided synthesis? To answer these questions, we conduct extensive experiments on several 2D human fashion datasets [11, 33, 67].

Datasets. We evaluate methods of 3D-aware clothed human generation on three real-world fashion datasets: MPV [11], DeepFashion [33] and UBCFashion [67]. They contain single clothed people in each image. We align and crop images according to the 2D human body keypoints, following [13]. Since we focus on human avatar generation, we use a segmentation model [8] to remove irrelevant backgrounds. We adopt an off-the-shelf pose estimator [27] to obtain approximate camera and SMPL parameters. We filter out images with partial observations and those with poor SMPL estimations, and get nearly 15K, 14K and 31K full-body images for each dataset, respectively. Horizontal-flip augmentation is used during training. We note these datasets are primarily composed of front-view images—few images captured from side or back views. To compensate this, we sample more side- and back-view images to re-balance viewpoint distributions following [2]. We will release pre-processed scripts and datasets. For more details, please refer to the appendix.

Table 1: Quantitative evaluation in terms of FID, depth, pose and warp accuracy on three datasets. Our AvatarGen outperforms all the baselines significantly.

	MPV				DeepFashion				UBCFashion			
	FID↓	Depth↓	Pose↓	Warp↓	FID↓	Depth↓	Pose↓	Warp↓	FID↓	Depth↓	Pose↓	Warp↓
GIRAFFE-HD	26.3	2.12	.099	31.4	25.3	1.94	.092	34.3	27.0	2.03	.094	35.2
StyleNeRF	10.7	1.46	.069	26.2	20.6	1.44	.067	22.8	15.9	1.43	.065	20.5
StyleSDF	29.5	1.74	.648	19.8	41.0	1.69	.613	20.4	35.9	1.76	.611	13.0
EG3D	18.6	1.52	.077	20.3	16.2	1.70	.065	14.8	17.7	1.66	.070	23.9
AvatarGen (Ours)	6.5	0.83	.050	4.7	9.6	0.86	.052	6.9	8.7	0.94	.059	6.0

4.1 Comparisons

Baselines. We compare our AvatarGen against four state-of-the-art methods for 3D-aware image synthesis: EG3D [2], StyleSDF [42], StyleNeRF [16] and GIRAFFE-HD [65]. All these methods combine volume renderer with 2D decoder for 3D-aware image synthesis. EG3D and StyleNeRF adopt progressive training to improve performance. StyleSDF uses SDF as geometry representation for regularized geometry modeling.

Quantitative evaluations. Tab. 1 provides quantitative comparisons between our AvatarGen and the baselines. We measure image quality with Fréchet Inception Distance (FID) [18] between 50k generated images and all of the available real images. We evaluate geometry quality by calculating Mean Squared Error (MSE) against pseudo groundtruth (GT) depth-maps (*Depth*) and poses (*Pose*) that are estimated from the generated images by [53, 27]. We also introduce an image warp metric (*Warp*) that warps side-view image with depth map to frontal view and computes MSE against the generated frontal-view image to further evaluate the geometry quality and multi-view consistency of the model. For additional evaluation details, please refer to the appendix. From Tab. 1, we observe our model outperforms all the baselines w.r.t. all the metrics and datasets. Notably, it outperforms baseline models by significant margins (69.5%, 63.1%, 64.0% in FID) on three datasets. These results clearly demonstrate its superiority in clothed human avatar synthesis. Moreover, it maintains state-of-the-art geometry quality, pose accuracy and multi-view consistency.

Qualitative results. We show a qualitative comparison against baselines in the left of Fig. 4. It can be observed that compared with our method, StyleSDF [42] generate 3D avatar with over-smoothed geometry and poor multi-view consistency. In addition, the noise and holes can be observed around the generated avatar and the geometry details like face and clothes are missing. EG3D [2] struggles to learn 3D human geometry from 2D images and suffers degenerated qualities. Compared with them, our AvatarGen generates 3D avatars with high-quality appearance with better view-consistency and geometric details.

4.2 Ablation studies

We conduct ablation studies on the Deepfashion dataset as its samples have diverse poses and appearances. We investigate effects of varying the following designs of AvatarGen.

Geometry proxy. Our AvatarGen uses signed distance field (SDF) as geometry proxy to regularize the geometry learning. To investigate its effectiveness, we also evaluate our model with density field as the proxy. As shown in Tab. 2a, if replacing SDF with density field, the quality of the generated avatars drops significantly—11.1% increase in FID, 38.6% and 66.8% increases in Depth and Warp metrics. This indicates SDF is important for the model to more precisely represent clothed human geometry. Without it, the model will produce noisy surface, and suffer performance drop.

Deformation schemes. Our model uses a pose-guided deformation to transform spatial points from the observation space to the canonical space. We also evaluate other two deformation schemes in Tab. 2b: 1) residual deformation [45, 44] only (*RD*), 2) inverse-skinning deformation [20] only (*IS*). When using RD only, the model training does not converge, indicating that learning deformation implicitly cannot handle large articulation of humans and lead to implausible results. While using IS only, the model achieves a reasonable result (FID: 10.7, Depth: 0.93, Warp: 7.7), verifying the importance of the explicitly pose-guided deformation. Further combining IS and RD (our model) boosts the performance sharply—10.3%, 7.5% and 10.4% decrease in FID, Depth and Warp metrics,

Table 2: Ablations on Deepfashion. In (e), *w/o* denotes without using SMPL body SDF prior, *Can.* or *Obs.* means using SDF prior from canonical or observation spaces.

<i>Geo.</i>				<i>Deform.</i>				<i>KNN</i>			
FID	Depth	Warp		FID	Depth	Warp		FID	Depth	Warp	
Density	10.8	1.40	20.8	RD	-	-	-	1	9.6	0.86	6.9
SDF	9.6	0.86	6.9	IS	10.7	0.93	7.7	2	10.4	0.90	7.4
(a) The effect of different geometry proxies.				IS+RD	9.6	0.86	6.9	3	13.1	1.08	10.2
				(b) Deformation schemes. IS and RD are inverse skinning and residual deformation.				4	16.3	1.14	15.3
<i>Ray Steps</i>	FID	Depth	Warp	<i>SDF Prior</i>				(c) Different number of KNN in inverse skinning deformation.			
12	12.4	1.04	7.7	FID	Depth	Warp		<i>SDF Scheme</i>	FID	Depth	Warp
24	10.7	0.92	7.5	w/o	14.3	1.12	8.3	Raw	10.8	0.94	7.9
36	10.0	0.89	7.2	Can.	10.4	0.89	7.5	Residual	9.6	0.86	6.9
48	9.6	0.86	6.9	Obs.	9.6	0.86	6.9	(f) SDF prediction schemes.			
(d) Number of ray steps.				(e) The effect of SMPL body SDF priors.							

respectively. Introducing the residual deformation to collaborate with the posed-guided inverse-skinning transformation indeed better represents non-rigid clothed human body deformation and thus our AvatarGen achieves better appearance and geometry modeling.

Number of KNN neighbors in inverse skinning deformation. For any spatial points, we use Nearest Neighbor to find the corresponding skinning weights for inverse skinning transformation (Eqn. (2)). More nearest neighbors can be used for obtaining skinning weights [31]. Thus, we study how the number of KNN affects model performance in Tab. 2c. We observe using more KNN neighbors gives worse performance. This is likely caused by 1) noisy skinning weights introduced by using more neighbors for calculation and 2) inaccurate SMPL estimation in data pre-processing step.

Number of ray steps. Tab. 2d shows the effect of the number of points sampled per ray for volume rendering. With only 12 sampled points for each ray, AvatarGen already achieves acceptable results, *i.e.*, 12.4, 1.04 and 7.7 in FID, Depth and Warp losses. With more sampling points, the performance monotonically increases, demonstrating the capacity of AvatarGen in 3D-aware avatars generation.

SMPL body SDF priors. AvatarGen adopts a SMPL-guided geometry learning scheme, *i.e.*, generating clothed human body SDFs on top of the coarse SMPL body mesh. As shown in Table 2e, if removing SMPL body guidance, the performance drops significantly, *i.e.*, 32.9%, 23.2%, 16.9% increase in FID, Depth and Warp losses. This indicates the coarse SMPL body information is important for guiding AvatarGen to better generate clothed human geometry. We also evaluate the performance difference between SMPL body SDFs queried from observation (*Obs.*) or canonical (*Can.*) spaces. We see the model guided by body SDFs queried from observation space obtains better performance as they are more accurate than the ones queried from the canonical space. Moreover, we study the effect of SMPL SDF regularization loss in Eqn. (8). If removing the regularization loss, the performance in all metrics drops (FID: 10.8 *vs.* 9.6, Depth: 0.96 *vs.* 0.86, Warp: 7.8 *vs.* 6.9), verifying the effectiveness of the proposed loss for regularized geometry learning.

SDF prediction schemes. Table 2f shows the effect of two SDF prediction schemes—predicting raw SDFs directly or SDF residuals on top of the coarse SMPL body SDFs. Compared with predicting the raw SDFs directly, the residual prediction scheme delivers better results, since it alleviates the geometry learning difficulties.

4.3 Applications

Single-view 3D reconstruction and re-pose. The right panel of Fig. 4 shows the application of our learned latent space for single-view 3D reconstruction. Following [2], we use pivotal tuning inversion (PTI) [52] to fit the target images (top) and recover both the appearance and the geometry (middle). With the recovered 3D representation and latent code, we can further use novel SMPL parameters (bottom) to re-pose/animate the human in the source images.

Text-guided synthesis. Recent works [46, 28] have shown that one could use a text-image embedding, such as CLIP [51], to guide StyleGAN2 for controlled synthesis. We also visualize text-guided clothed human synthesis in Fig. 5. Specifically, we use StyleCLIP [46] to manipulate a synthesized image with a sequence of text prompts. The optimization based StyleCLIP is used as it is flexible for any input text. From the figure, our AvatarGen is able to synthesis different style human images given



Figure 4: (Left) Qualitative comparison of multi-view rendering and geometry quality against baselines including EG3D [2] and StyleSDF [42]. (Right) Single-view 3D reconstruction and reanimation result of AvatarGen. Given source image, we reconstruct both color and geometry of the human in the image. The re-pose step further takes novel SMPL parameters as input and animates the reconstructed avatar.



Figure 5: Text-guided (left) synthesis results of AvatarGen with multi-view rendering (right).

different text prompts. This clearly indicates that AvatarGen can be an effective tool for text-guided portrait synthesis where detailed descriptions are provided.

5 Conclusion

This work introduced the first 3D-aware human avatar generative model, AvatarGen. By factorizing the generative process into the canonical avatar generation and deformation stages, AvatarGen can leverage the geometry prior and effective tri-plane representation to address the challenges in animatable human avatar generation. We demonstrated AvatarGen can generate clothed human avatars with arbitrary poses and viewpoints. Besides, it can also generate avatars from multi-modality input conditions, like natural language description and 2D images (for inverting). This work substantially extends the 3D generative models from objects of simple structures (e.g., human faces, rigid objects) to articulated and complex objects. We believe this model will make the creation of human avatars more accessible to ordinary users, assist designers and reduce the manual cost.

References

- [1] Panos Achlioptas, Olga Diamanti, Ioannis Mitliagkas, and Leonidas Guibas. Learning representations and generative models for 3d point clouds. In *ICML*, 2018.
- [2] Eric R Chan, Connor Z Lin, Matthew A Chan, Koki Nagano, Boxiao Pan, Shalini De Mello, Orazio Gallo, Leonidas Guibas, Jonathan Tremblay, Sameh Khamis, et al. Efficient geometry-aware 3d generative adversarial networks. *CVPR*, 2022.
- [3] Eric R Chan, Marco Monteiro, Petr Kellnhofer, Jiajun Wu, and Gordon Wetzstein. pi-gan: Periodic implicit generative adversarial networks for 3d-aware image synthesis. In *CVPR*, 2021.
- [4] Jianchuan Chen, Ying Zhang, Di Kang, Xuefei Zhe, Linchao Bao, Xu Jia, and Huchuan Lu. Animatable neural radiance fields from monocular rgb videos. *arXiv*, 2021.
- [5] Mingfei Chen, Jianfeng Zhang, Xiangyu Xu, Lijuan Liu, Yujun Cai, Jiashi Feng, and Shuicheng Yan. Geometry-guided progressive nerf for generalizable and efficient neural human rendering. *arXiv*, 2021.
- [6] Zhiqin Chen and Hao Zhang. Learning implicit fields for generative shape modeling. In *CVPR*, 2019.
- [7] Alvaro Collet, Ming Chuang, Pat Sweeney, Don Gillett, Dennis Evseev, David Calabrese, Hugues Hoppe, Adam Kirk, and Steve Sullivan. High-quality streamable free-viewpoint video. In *ACM Trans. on Graphics*, 2015.
- [8] PaddlePaddle Contributors. Paddleseg, end-to-end image segmentation kit based on paddlepaddle. <https://github.com/PaddlePaddle/PaddleSeg>, 2019.
- [9] Paul Debevec, Tim Hawkins, Chris Tchou, Haarm-Pieter Duiker, Westley Sarokin, and Mark Sagar. Acquiring the reflectance field of a human face. In *Proceedings of the 27th annual conference on Computer graphics and interactive techniques*, 2000.
- [10] Yu Deng, Jiaolong Yang, Jianfeng Xiang, and Xin Tong. Gram: Generative radiance manifolds for 3d-aware image generation. *CVPR*, 2022.
- [11] Haoye Dong, Xiaodan Liang, Xiaohui Shen, Bochao Wang, Hanjiang Lai, Jia Zhu, Zhiting Hu, and Jian Yin. Towards multi-pose guided virtual try-on network. In *ICCV*, 2019.
- [12] Mingsong Dou, Sameh Khamis, Yury Degtyarev, Philip Davidson, Sean Ryan Fanello, Adarsh Kowdle, Sergio Orts Escolano, Christoph Rhemann, David Kim, Jonathan Taylor, et al. Fusion4d: Real-time performance capture of challenging scenes. In *ACM Trans. on Graphics*, 2016.
- [13] Jianglin Fu, Shikai Li, Yuming Jiang, Kwan-Yee Lin, Chen Qian, Chen-Change Loy, Wayne Wu, and Ziwei Liu. Stylegan-human: A data-centric odyssey of human generation. *arXiv*, 2022.
- [14] Thiago L. Gomes, Thiago M. Coutinho, Rafael Azevedo, Renato Martins, and Erickson R. Nascimento. Creating and reenacting controllable 3d humans with differentiable rendering. In *WACV*, 2022.
- [15] Ian Goodfellow, Jean Pouget-Abadie, Mehdi Mirza, Bing Xu, David Warde-Farley, Sherjil Ozair, Aaron Courville, and Yoshua Bengio. Generative adversarial nets. In *NeurIPS*, 2014.
- [16] Jiatao Gu, Lingjie Liu, Peng Wang, and Christian Theobalt. Stylenerf: A style-based 3d-aware generator for high-resolution image synthesis. *CVPR*, 2022.
- [17] Kaiwen Guo, Peter Lincoln, Philip Davidson, Jay Busch, Xueming Yu, Matt Whalen, Geoff Harvey, Sergio Orts-Escolano, Rohit Pandey, Jason Dourgarian, et al. The relightables: Volumetric performance capture of humans with realistic relighting. In *ACM Trans. on Graphics*, 2019.
- [18] Martin Heusel, Hubert Ramsauer, Thomas Unterthiner, Bernhard Nessler, and Sepp Hochreiter. Gans trained by a two time-scale update rule converge to a local nash equilibrium. *NeurIPS*, 2017.
- [19] Fangzhou Hong, Mingyuan Zhang, Liang Pan, Zhongang Cai, Lei Yang, and Ziwei Liu. Avatarclip: Zero-shot text-driven generation and animation of 3d avatars. *ACM Trans. on Graphics*, 2022.
- [20] Zeng Huang, Yuanlu Xu, Christoph Lassner, Hao Li, and Tony Tung. Arch: Animatable reconstruction of clothed humans. In *CVPR*, 2020.
- [21] Alec Jacobson, Ilya Baran, Ladislav Kavan, Jovan Popović, and Olga Sorkine. Fast automatic skinning transformations. *ACM Trans. on Graphics*, 2012.

- [22] Boyi Jiang, Yang Hong, Hujun Bao, and Juyong Zhang. Selfrecon: Self reconstruction your digital avatar from monocular video. In *CVPR*, 2022.
- [23] Tero Karras, Timo Aila, Samuli Laine, and Jaakko Lehtinen. Progressive growing of GANs for improved quality, stability, and variation. In *ICCV*, 2018.
- [24] Tero Karras, Miika Aittala, Samuli Laine, Erik Härkönen, Janne Hellsten, Jaakko Lehtinen, and Timo Aila. Alias-free generative adversarial networks. In *NeurIPS*, 2021.
- [25] Tero Karras, Samuli Laine, and Timo Aila. A style-based generator architecture for generative adversarial networks. In *CVPR*, 2019.
- [26] Tero Karras, Samuli Laine, Miika Aittala, Janne Hellsten, Jaakko Lehtinen, and Timo Aila. Analyzing and improving the image quality of StyleGAN. In *CVPR*, 2020.
- [27] Nikos Kolotouros, Georgios Pavlakos, Michael J Black, and Kostas Daniilidis. Learning to reconstruct 3d human pose and shape via model-fitting in the loop. In *ICCV*, 2019.
- [28] Gihyun Kwon and Jong Chul Ye. Clipstyler: Image style transfer with a single text condition. In *Proceedings of the IEEE/CVF Conference on Computer Vision and Pattern Recognition*, pages 18062–18071, 2022.
- [29] Ruihui Li, Xianzhi Li, Chi-Wing Fu, Daniel Cohen-Or, and Pheng-Ann Heng. Pu-gan: a point cloud upsampling adversarial network. In *ICCV*, 2019.
- [30] Yiyi Liao, Katja Schwarz, Lars Mescheder, and Andreas Geiger. Towards unsupervised learning of generative models for 3D controllable image synthesis. In *CVPR*, 2020.
- [31] Lingjie Liu, Marc Habermann, Viktor Rudnev, Kripasindhu Sarkar, Jiatao Gu, and Christian Theobalt. Neural actor: Neural free-view synthesis of human actors with pose control. *ACM Trans. on Graphics*, 2021.
- [32] Ting Liu, Jianfeng Zhang, Xuecheng Nie, Yunchao Wei, Shikui Wei, Yao Zhao, and Jiashi Feng. Spatial-aware texture transformer for high-fidelity garment transfer. In *IEEE Trans. on Image Processing*, 2021.
- [33] Ziwei Liu, Ping Luo, Shi Qiu, Xiaogang Wang, and Xiaoou Tang. Deepfashion: Powering robust clothes recognition and retrieval with rich annotations. In *CVPR*, 2016.
- [34] Matthew Loper, Naureen Mahmood, Javier Romero, Gerard Pons-Moll, and Michael J Black. Smpl: A skinned multi-person linear model. *ACM Trans. on Graphics*, 2015.
- [35] Lars Mescheder, Andreas Geiger, and Sebastian Nowozin. Which training methods for gans do actually converge? In *International conference on machine learning*, pages 3481–3490. PMLR, 2018.
- [36] Lars Mescheder, Michael Oechsle, Michael Niemeyer, Sebastian Nowozin, and Andreas Geiger. Occupancy networks: Learning 3d reconstruction in function space. In *CVPR*, 2019.
- [37] Ben Mildenhall, Pratul P Srinivasan, Matthew Tancik, Jonathan T Barron, Ravi Ramamoorthi, and Ren Ng. Nerf: Representing scenes as neural radiance fields for view synthesis. In *ECCV*, 2020.
- [38] Thu Nguyen-Phuoc, Chuan Li, Lucas Theis, Christian Richardt, and Yong-Liang Yang. HoloGAN: Unsupervised learning of 3D representations from natural images. In *ICCV*, 2019.
- [39] Thu Nguyen-Phuoc, Christian Richardt, Long Mai, Yong-Liang Yang, and Niloy Mitra. BlockGAN: Learning 3D object-aware scene representations from unlabelled images. In *NeurIPS*, 2020.
- [40] Michael Niemeyer and Andreas Geiger. Giraffe: Representing scenes as compositional generative neural feature fields. In *CVPR*, 2021.
- [41] Atsuhiko Noguchi, Xiao Sun, Stephen Lin, and Tatsuya Harada. Neural articulated radiance field. In *ICCV*, 2021.
- [42] Roy Or-El, Xuan Luo, Mengyi Shan, Eli Shechtman, Jeong Joon Park, and Ira Kemelmacher-Shlizerman. Stylesdf: High-resolution 3d-consistent image and geometry generation. *CVPR*, 2022.
- [43] Jeong Joon Park, Peter Florence, Julian Straub, Richard Newcombe, and Steven Lovegrove. Deepsdf: Learning continuous signed distance functions for shape representation. In *CVPR*, 2019.
- [44] Keunhong Park, Utkarsh Sinha, Jonathan T Barron, Sofien Bouaziz, Dan B Goldman, Steven M Seitz, and Ricardo Martin-Brualla. Deformable neural radiance fields. *arXiv*, 2020.

- [45] Keunhong Park, Utkarsh Sinha, Jonathan T Barron, Sofien Bouaziz, Dan B Goldman, Steven M Seitz, and Ricardo Martin-Brualla. Nerfies: Deformable neural radiance fields. In *ICCV*, 2021.
- [46] Or Patashnik, Zongze Wu, Eli Shechtman, Daniel Cohen-Or, and Dani Lischinski. Styleclip: Text-driven manipulation of stylegan imagery. In *ICCV*, 2021.
- [47] Sida Peng, Juntong Dong, Qianqian Wang, Shangzhan Zhang, Qing Shuai, Hujun Bao, and Xiaowei Zhou. Animatable neural radiance fields for human body modeling. *ICCV*, 2021.
- [48] Sida Peng, Shangzhan Zhang, Zhen Xu, Chen Geng, Boyi Jiang, Hujun Bao, and Xiaowei Zhou. Animatable neural implicit surfaces for creating avatars from videos. *arXiv*, 2022.
- [49] Sida Peng, Yuanqing Zhang, Yinghao Xu, Qianqian Wang, Qing Shuai, Hujun Bao, and Xiaowei Zhou. Neural body: Implicit neural representations with structured latent codes for novel view synthesis of dynamic humans. In *CVPR*, 2021.
- [50] Albert Pumarola, Enric Corona, Gerard Pons-Moll, and Francesc Moreno-Noguer. D-nerf: Neural radiance fields for dynamic scenes. In *CVPR*, 2021.
- [51] Alec Radford, Jong Wook Kim, Chris Hallacy, Aditya Ramesh, Gabriel Goh, Sandhini Agarwal, Girish Sastry, Amanda Askell, Pamela Mishkin, Jack Clark, et al. Learning transferable visual models from natural language supervision. In *ICML*, 2021.
- [52] Daniel Roich, Ron Mokady, Amit H Bermano, and Daniel Cohen-Or. Pivotal tuning for latent-based editing of real images. *ACM Trans. on Graphics*, 2021.
- [53] Shunsuke Saito, Tomas Simon, Jason Saragih, and Hanbyul Joo. Pifuhd: Multi-level pixel-aligned implicit function for high-resolution 3d human digitization. In *CVPR*, 2020.
- [54] Katja Schwarz, Yiyi Liao, Michael Niemeyer, and Andreas Geiger. Graf: Generative radiance fields for 3d-aware image synthesis. *NeurIPS*, 2020.
- [55] Shih-Yang Su, Frank Yu, Michael Zollhöfer, and Helge Rhodin. A-nerf: Articulated neural radiance fields for learning human shape, appearance, and pose. In *NeurIPS*, 2021.
- [56] Zhuo Su, Lan Xu, Zerong Zheng, Tao Yu, Yebin Liu, and Lu Fang. Robustfusion: Human volumetric capture with data-driven visual cues using a rgb-d camera. In *ECCV*, 2020.
- [57] Attila Szabó, Givi Meishvili, and Paolo Favaro. Unsupervised generative 3D shape learning from natural images. *arXiv*, 2019.
- [58] Ayush Tewari, MalliKarjun B R, Xingang Pan, Ohad Fried, Maneesh Agrawala, and Christian Theobalt. Disentangled3d: Learning a 3d generative model with disentangled geometry and appearance from monocular images. In *CVPR*, 2022.
- [59] Peng Wang, Lingjie Liu, Yuan Liu, Christian Theobalt, Taku Komura, and Wenping Wang. Neus: Learning neural implicit surfaces by volume rendering for multi-view reconstruction. *NeurIPS*, 2021.
- [60] Chung-Yi Weng, Brian Curless, Pratul P. Srinivasan, Jonathan T. Barron, and Ira Kemelmacher-Shlizerman. HumanNeRF: Free-viewpoint rendering of moving people from monocular video. *CVPR*, 2022.
- [61] Jiajun Wu, Chengkai Zhang, Tianfan Xue, William T. Freeman, and Joshua B. Tenenbaum. Learning a probabilistic latent space of object shapes via 3D generative-adversarial modeling. In *NeurIPS*, 2016.
- [62] Donglai Xiang, Fabian Prada, Timur Bagautdinov, Weipeng Xu, Yuan Dong, He Wen, Jessica Hodgins, and Chenglei Wu. Modeling clothing as a separate layer for an animatable human avatar. *ACM Trans. on Graphics*, 2021.
- [63] Hongyi Xu, Thiemo Alldieck, and Cristian Sminchisescu. H-nerf: Neural radiance fields for rendering and temporal reconstruction of humans in motion. *NeurIPS*, 2021.
- [64] Xiangyu Xu and Chen Change Loy. 3D human texture estimation from a single image with transformers. In *ICCV*, 2021.
- [65] Yang Xue, Yuheng Li, Krishna Kumar Singh, and Yong Jae Lee. Giraffe hd: A high-resolution 3d-aware generative model. In *CVPR*, 2022.
- [66] Lior Yariv, Jiatao Gu, Yoni Kasten, and Yaron Lipman. Volume rendering of neural implicit surfaces. In *NeurIPS*, 2021.

- [67] Polina Zablotzkaia, Aliaksandr Siarohin, Bo Zhao, and Leonid Sigal. Dwnet: Dense warp-based network for pose-guided human video generation. *BMVC*, 2019.
- [68] Jiakai Zhang, Xinhang Liu, Xinyi Ye, Fuqiang Zhao, Yanshun Zhang, Minye Wu, Yingliang Zhang, Lan Xu, and Jingyi Yu. Editable free-viewpoint video using a layered neural representation. *ACM Trans. on Graphics*, 2021.
- [69] Jiakai Zhang, Liao Wang, Xinhang Liu, Fuqiang Zhao, Minzhang Li, Haizhao Dai, Boyuan Zhang, Wei Yang, Lan Xu, and Jingyi Yu. Neuvv: Neural volumetric videos with immersive rendering and editing. *ACM Trans. on Graphics*, 2022.